AD-A062 090 HONEYWELL CORPORATE MATERIAL SCIENCES CENTER BLOOMIN--ETC F/G 17/1
STRESS RELAXATION IN PZT.(U)
OCT 78 B G KOEPKE, K A ESAKLUL, W W GERBERICH N00014-76-C-0625
UNCLASSIFIED TR-2 NL

| OF |
AD
A062090

END
DATE
FILMED
3-79
DDC

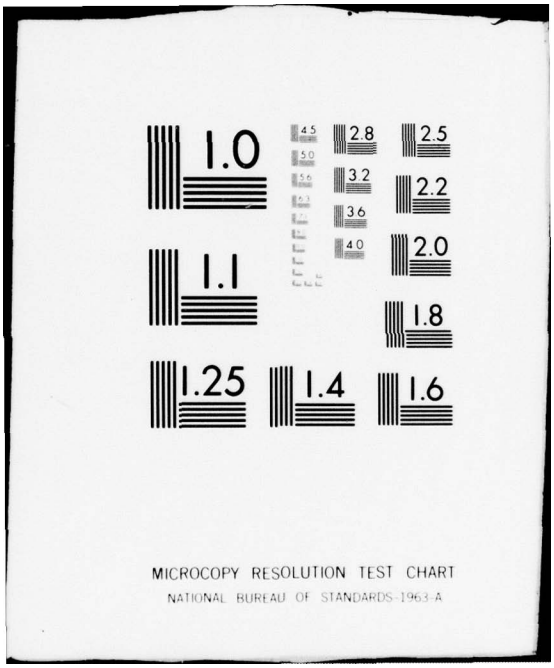
1.0
1.1
1.25
1.4
1.6
1.8
2.0
2.2
2.5
2.8
3.2
3.6
4.0
4.5
5.0
MICROCOPY RESOLUTION TEST CHART
NATIONAL BUREAU OF STANDARDS-1963-A

code 471
NR032-562

LEVEL II

12

DDC FILE COPY AD A062090

STRESS RELAXATION IN PZT

Second Technical Report

by

B. G. Koepke, K. A. Esaklul and W. W. Gerberich*

Honeywell Corporate Material Sciences Center

Office of Naval Research Project CG103

Contract No. N00014-76-C-0625/P00002

October 1978

DISTRIBUTION STATEMENT A
Approved for public release;
Distribution Unlimited

DDC
RECEIVED
DEC 12 1978
A

Honeywell Inc.
Corporate Material Sciences Center
10701 Lyndale Avenue South
Bloomington, Minnesota 55420

*University of Minnesota

Department of Material Science and Chemical Engineering

41365
78 11 24 036

STRESS RELAXATION IN PZT.

Second Technical Report

by

B. G. Koepke, K. A. Esaklul and W. W. Gerberich*

Honeywell Corporate Material Sciences Center

Office of Naval Research Project CG103

Contract No. N00014-76-C-0625/P00002

October 1978

TR-2

41 p.

Honeywell Inc.
Corporate Material Sciences Center
10701 Lyndale Avenue South
Bloomington, Minnesota 55420

*University of Minnesota

Department of Material Science and Chemical Engineering

41365

410336

PRECEDING PAGE BLANK-NOT FILMED

ABSTRACT

Time-dependent deformation in the sonar transducer ceramic, PZT, has been studied by stress relaxation techniques. Logarithmic stress relaxation was not observed but the data could be treated in terms of an analysis of thermally activated deformation due to Reed-Hill and Dahlberg. The room temperature activation energy and activation volume of the rate-controlling deformation mechanism were measured to be 25 kcal/mole and 7,000Å^3, respectively. A dislocation model of the domain processes responsible for deformation is presented that is consistent with the experimental data.

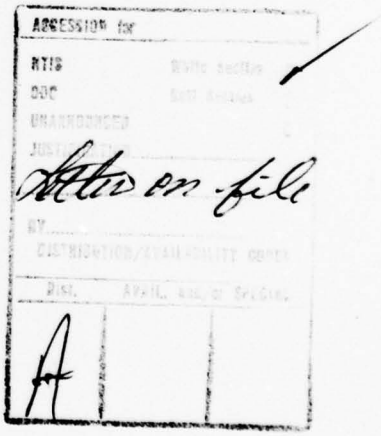

PRECEDING PAGE BLANK-NOT FILMED

CONTENTS

Section		Page
I	INTRODUCTION	1
II	EXPERIMENTAL PROCEDURE	3
III	RESULTS	8
IV	ANALYSIS OF STRESS RELAXATION DATA	11
V	A MODEL OF TIME-DEPENDENT DEFORMATION IN PZT	22
VI	CONCLUSIONS	26
VII	ACKNOWLEDGEMENTS	27
VIII	REFERENCES	28

78 11 24 036

LIST OF ILLUSTRATIONS

Figure		Page
1	Photomicrograph Showing Microstructure of PZT	4
2	Curves Showing the Effect of Machine Relaxation on Stress Relaxation Data	6
3	Schematic Showing Incremental Unloading Technique for Internal Stress Measurement[11]	7
4	Stress Relaxation Data for PZT Taken From Two Initial Stress Levels at Room Temperature	9
5	Stress Relaxation Data for PZT Taken From an Initial Stress Level of Approximately 65.5 MPa at 71°C	10
6	Variation of the Internal Stress as Measured by the Incremental Unloading Technique From an Initial Stress Level of 65.5 MPa With Temperature	17
7	Log Tanh $(\frac{\beta\sigma^*}{2RT})$ Plotted as a Function of Time at Two Temperatures	18
8	Temperature Dependence of the Activation Volume Measured From Stress Relaxation Data Taken From an Initial Stress of 65.5 MPa	19
9	Activation Volume for PZT Plotted as a Function of the Effective Stress at Room Temperature	20
10	Log $\frac{\tau\epsilon\beta}{T}$ Plotted versus $\frac{1}{T}$ for PZT	21
11	Schematic Showing the Geometry of Twinning in PZT	24

I. INTRODUCTION

When $BaTiO_3$ and other piezoelectric ceramics are subjected to an applied stress a large part of the resulting strain is time dependent and reversible.[1-5] This anelastic[6] component of the deformation is generally attributed to domain processes-specifically the stress-induced migration of non-180-degree domain boundaries. There are a number of reasons why non-180-degree domain processes are considered to be responsible for the deformation. First, there is no strain associated with the migration of a 180-degree domain boundary.[2,7] Second, time-dependent deformation is absent above the Curie temperature.[2,3] Finally, time-dependent deformation has been shown to be eliminated in $BaTiO_3$ single crystals if the crystals are deformed to a strain at which all 90-degree domain boundaries have migrated out of the crystal.

We should point out at this time that studies of the relation of domain processes to deformation in piezoelectric ceramics have practical significance. This is due to the relation between deformation, domain processes and aging; i.e., the degradation of the properties of a poled specimen with time. It is generally concluded that the net polarization of a poled piezoelectric ceramic decreases with time after poling due to domain processes, specifically the stress-induced migration of domain boundaries.

Time-dependent deformation in piezoelectric ceramics is known to depend on stress and temperature.[1,2] Thus, a study of the kinetics of deformation in these materials should yield information relating to the deformation mechanism itself. A number of marginally successful attempts to relate the kinetics of time-dependent deformation in piezoelectric ceramics to domain processes have been made. Syrkin and Elgard[2] analyzed the time dependence of the anelastic strain under constant stress of a number of

piezoelectric ceramics in terms of an exponential function. For two $BaTiO_3$ compositions, relaxation times on the order of ten minutes were determined and an activation energy of about 7.5 kcal/mole was measured. Relaxation times measured on a Sr and Nb-modified PZT ceramic were too small to analyze. Relaxation was attributed to 90-degrees domain boundary migration but a detailed mechanism was not discussed. Other studies of time-dependent deformation have been based on stress relaxation tests in which the stress was measured as a function of time at constant strain. Prasad and Subbarao[5] studied stress relaxation in $BaTiO_3$ single crystals at room temperature and concluded that time-dependent deformation was due to 90-degree domain boundary motion. When the stress relaxation data were analyzed in terms of a logarithmic and an exponential function, however, a fit was only obtained in both cases over a short time span. No attempts were made to obtain activation parameters.

In this report we present the results of a study of the kinetics of time-dependent deformation in PZT based on stress relaxation measurements. To the authors' knowledge stress relaxation data in this material have not been reported or discussed previously. In agreement with data on $BaTiO_3$,[5] a logarithmic time dependence of the stress was not observed over the time period examined. The results could, however, be treated in terms of a known kinetic analysis and the activation parameters of the deformation mechanism were determined. A dislocation model of the domain processes responsible for deformation in PZT is presented that is consistent with the measured activation parameters.

II. EXPERIMENTAL PROCEDURE

The PZT used in this study is the same as that used in privious work[9,10] and is a Navy Type III high-drive sonar ceramic* with a nominal composition of $Pb_{0.94}Sr_{0.06}Ti_{0.47}Zr_{0.53}O_3$ plus proprietary additions. The composition has been confirmed by x-ray measurements in our laboratory to be tetragonal below the Curie temperature and is dielectrically "hard". The material is produced by cold isostatic pressing and sintering and is approximately 94 percent dense. A micrograph illustrating the fine-grained, equiax microstructure of this material is shown in Figure 1. The grain size is approximately 4μm.

Test bars for stress relaxation tests were cut from sintered transducer tubes with a diamond slicing wheel and were surface ground in the long dimensions of the bars with a 100-grit diamond wheel. All cutting and grinding was carried out wet. The test bars were 50.8mm (2 inches) long, 5.08mm (0.2 inch) wide and 1.78mm (0.07 inch) thick and were tested in three-point bending in a table model testing machine** over a span of 43.2mm (1.7 inches). All specimens tested were in the unpoled condition. Elevated temperature tests were run with the specimens immersed in a heated bath*** maintained to ± 2°C. Before any test was run at an elevated temperature, the specimen and loading fixture were kept at temperature for at least 5 hours to allow thermal equilibrium to be approached.

---

*Honeywell Ceramics Center, Golden Valley, MN

**Instron Corp., Canton, MA

***3M Fluorinert Electronic Liquid FC-30

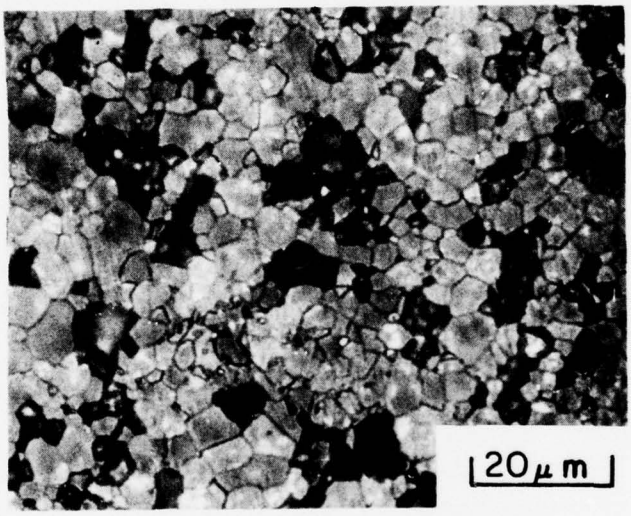

Figure 1. Photomicrograph Showing Microstructure of PZT.

Stress relaxation measurements were made by loading the specimen at a cross-head speed of 0.025 mm/min (0.001 inch/min) to a predetermined load, stopping the crosshead, and recording the load as a function of time. Prior to each run the background relaxation of the system was measured with a rigid alumina specimen in place and subsequently subtracted from the relaxation curve of the specimen as shown in Figure 2.

Internal stress measurements were made using the incremental unloading technique of McEwen et al.[11] In this technique the stress relaxation over a finite time internal (e.g., 1 min) is measured at a number of initial stress levels as shown schematically in Figure 3. At stress levels below the internal stress level indicated on Figure 3 as σ_i, the relaxation is negative. The internal stress represents the inherent resistance of the material to deformation and opposes the applied stress acting on the rate-controlling deformation mechanism.[11,12]

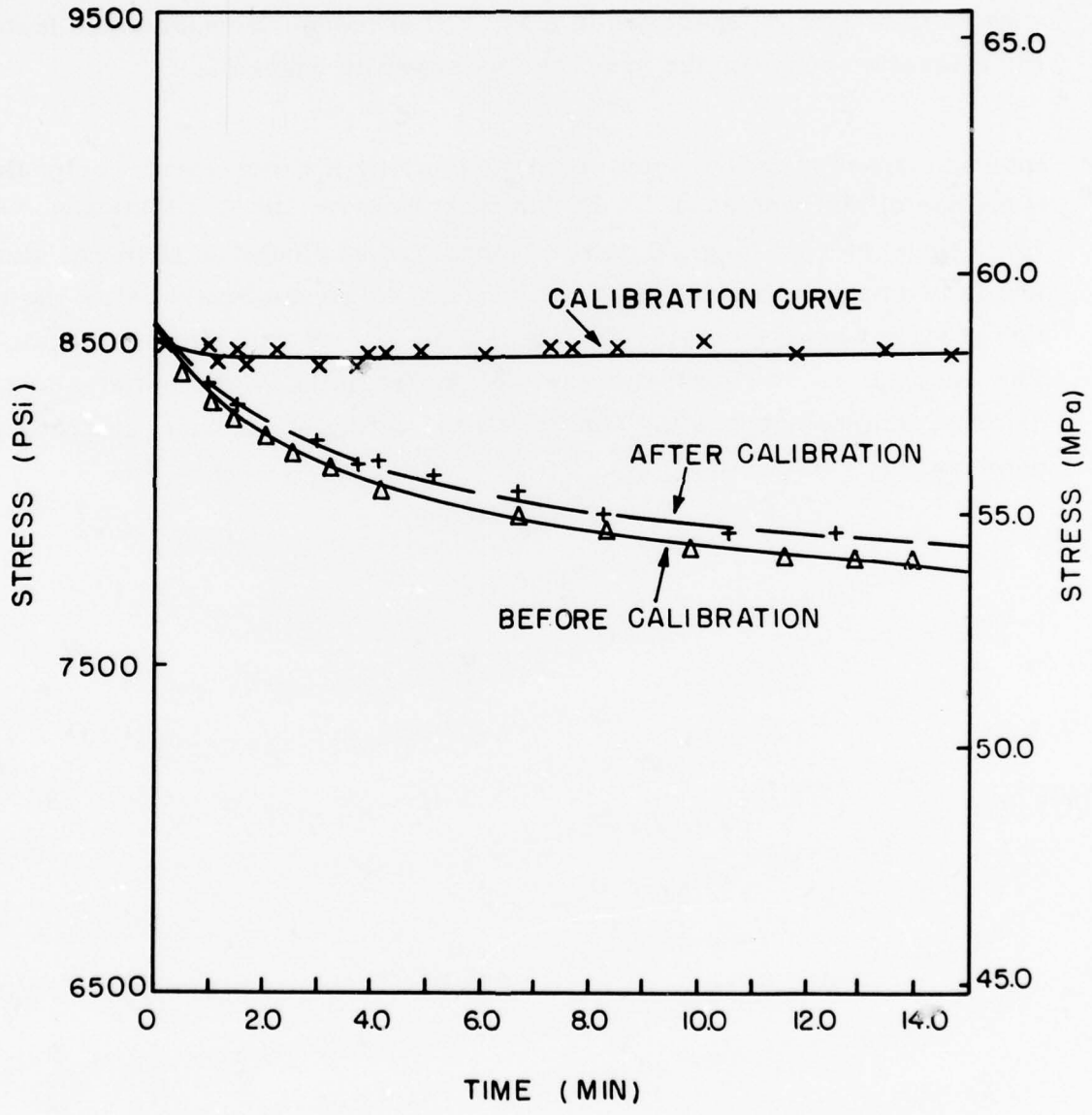

Figure 2. Curves Showing the Effect of Machine Relaxation on Stress Relaxation Data

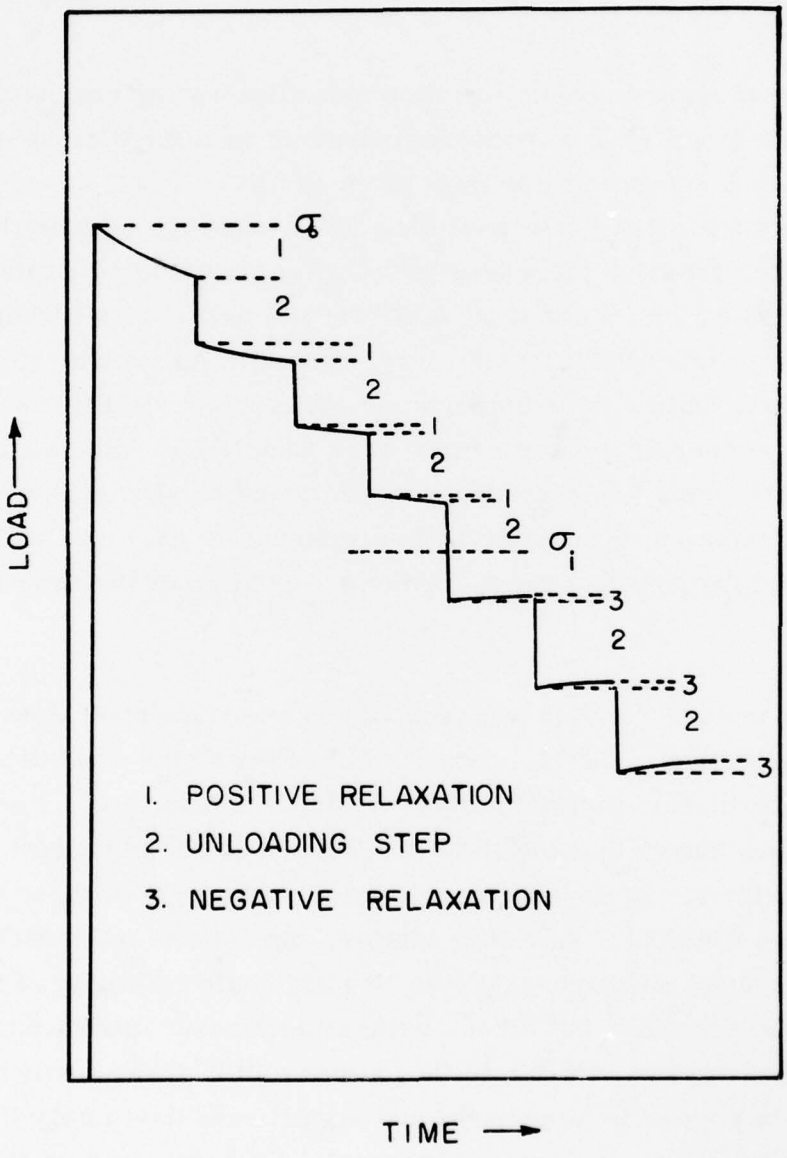

Figure 3. Schematic Showing Incremental Unloading Technique for Internal Stress Measurement[11]

III. RESULTS

Figure 4 shows stress versus log time data illustrating typical stress relaxation behavior of PZT at room temperature as a function of initial stress level. Figure 5 shows similar data taken at 71°C. In all cases the curves are corrected for machine relaxation. The data taken at room temperature show that the relaxation increases with initial stress and that data taken from an initial stress of about 65.5 MPa (9500 psi) at room temperature and 71°C show that relaxation also increases with temperature. Note the change in scale on the high-temperature curve shown in Figure 5. The highest test temperature used in this work was 71°C. Anomalous mechanical effects are observed in many instances at higher temperatures as the Curie temperature is approached. In all cases the data exhibit linear stress versus log time behavior over only a portion of the time span of the test.

Attempts to analyze the data with respect to an exponential time dependence were similarly unsuccessful. According to Zener[6] the time dependence of anelastic deformation in most solids should be exponential. Furthermore, experience has shown that the time dependence of deformation in plastically deformed materials is usually logarithmic.[12] Neither of these were found to be the case for PZT. As noted earlier, the results on $BaTiO_3$ are unclear. Data taken on polycrystalline $BaTiO_3$ could be analyzed in terms of an exponential function[2] but stress relaxation measurements on single crystals exhibited results similar to those shown in Figures 4 and 5 for PZT. These results appear to be general and significant; they imply that straightforward kinetic analyses developed to explain exponential and logarithmic time-dependent deformation[2,6,12] cannot be applied to stress relaxation data on piezoelectric ceramics. There is, however, an analysis of thermally activated deformation that can be applied to the data shown in Figures 4 and 5. The analysis is discussed in Section IV.

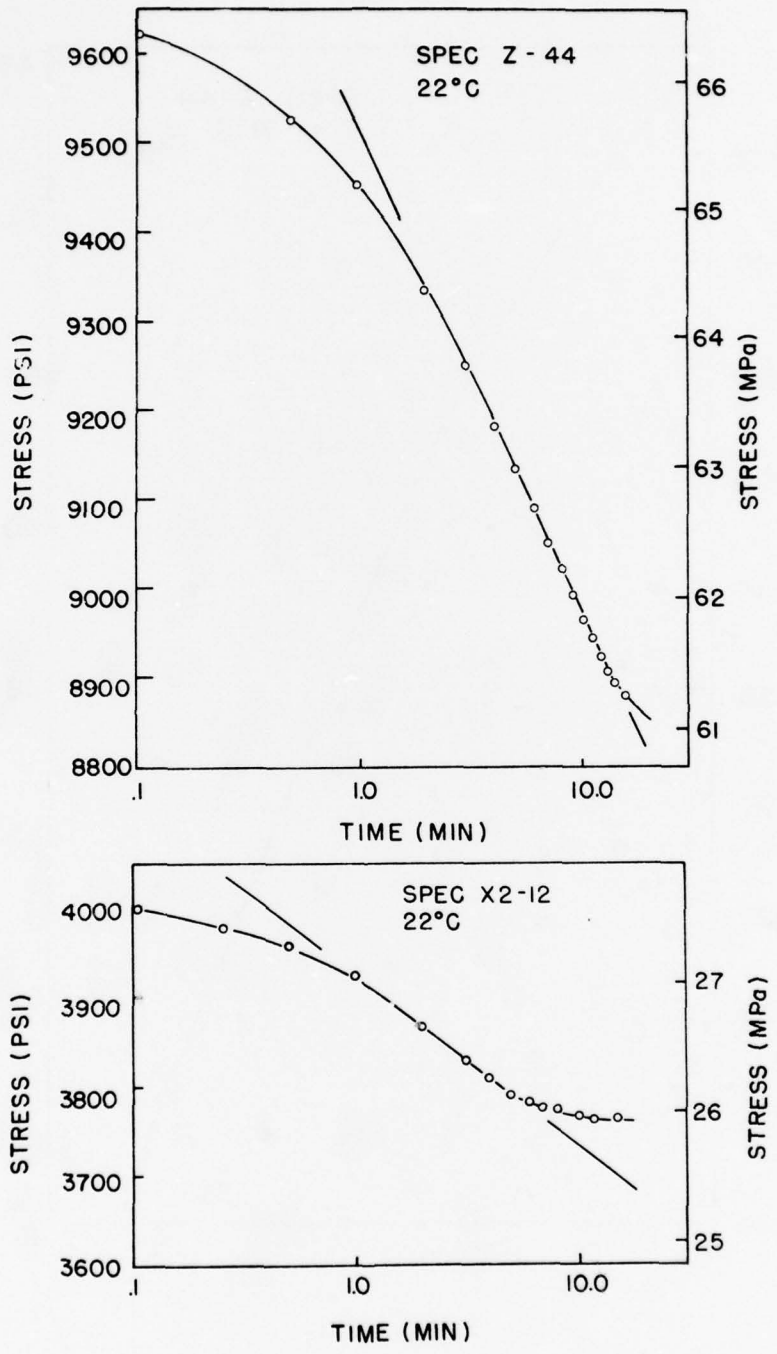

Figure 4. Stress Relaxation Data for PZT Taken From Two Initial Stress Levels at Room Temperature

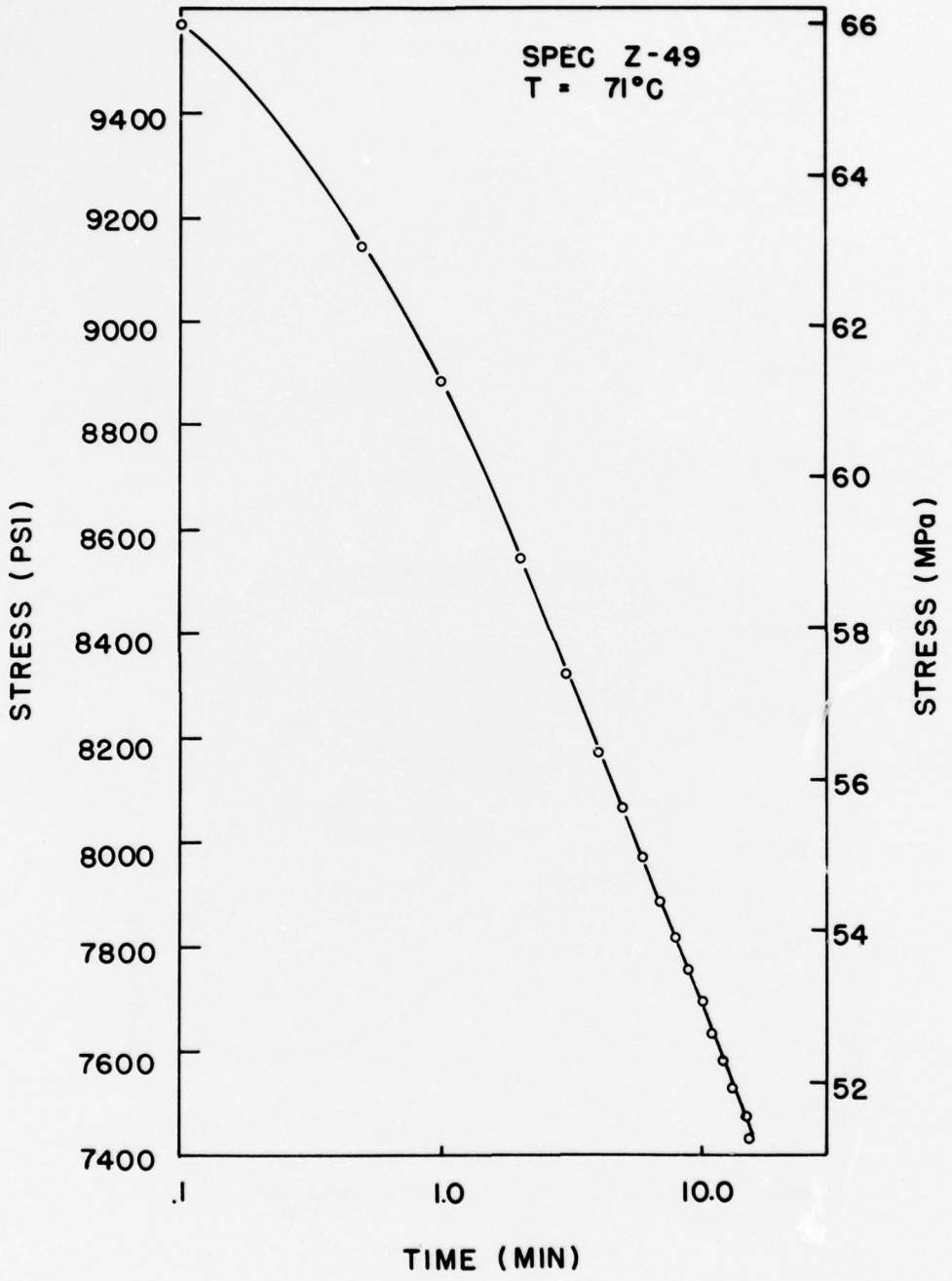

Figure 5. Stress Relaxation Data for PZT Taken From an Initial Stress Level of Approximately 65.5 MPa at 71°C

IV. ANALYSIS OF STRESS RELAXATION DATA

Stress relaxation is a function of both stress and temperature and can be discussed in terms of the theory of thermally activated deformation of crystalline solids.[12] Since the concepts of thermally activated deformation have been extensively developed and well documented,[13-15] they will be only briefly discussed here. Plastic and anelastic deformation of crystalline solids are known to be thermally activated processes which depend on time, temperature and stress.[6, 12-15] In all cases deformation occurs by the activation (by stress and/or temperature) of some local deformation mechanism over an obstacle. The rates at which the obstacles are surmounted during deformation define the kinetics of the process, i.e., the strain rate. Thus, the kinetics of deformation can be studied by measuring the relations between the strain rate, stress, and temperature. Stress relaxation measurements are one way of obtaining this information.[12]

During a stress relaxation test under fixed grip conditions the change in the total strain is zero. Thus if machine extensions are neglected

$$\varepsilon_{tot} = \varepsilon_{el} + \varepsilon^* = 0$$

where ε_{tot} is the total strain, ε_{el} is the elastic strain and ε^* is the inelastic (anelastic plus plastic) strain in the specimen. During relaxation the strain rates are related to the stress rates by

$$\dot{\varepsilon}_{el} + \dot{\varepsilon}^* = -\frac{\dot{\sigma}}{M} \simeq 0.$$

where M is a term containing the specimen dimensions and machine stiffness and is assumed to be large. Since the elastic strain rate is

$$\dot{\varepsilon}_{el} = \frac{\dot{\sigma}}{M_u}$$

where M_u is the unrelaxed modulus, the inelastic strain rate can be written[12]

$$\dot{\varepsilon}^* = -\frac{\dot{\sigma}}{M_u}$$

The stress can be written as the sum of an unrelaxed stress, σ_G, and a relaxable stress σ^*

$$\sigma = \sigma_G + \sigma^*$$

where $\sigma_G = \sigma$ at $t = \infty$. In thermally activated deformation σ_G represents long-range internal stresses in the material that oppose activation of the local deformation mechanism.[12, 13] The long-range stresses are relatively insensitive to strain rate and depend on temperature only through the shear modulus, G. Thus the relaxable strain rate can be written in terms of the relaxable stress rate by

$$\dot{\varepsilon}^* = -\frac{\dot{\sigma}^*}{M_u} \tag{1}$$

if machine relaxations are neglected.

Providing that a single mechanism is rate controlling, the inelastic strain rate during thermally activated deformation in PZT can be written as an Ahrennius equation[13, 14]

$$\dot{\varepsilon}^* = Ae^{-\frac{(Q - V\tau^*)}{RT}} \tag{2}$$

where the pre-exponential factor, A, contains an entropy term and has dimensions of frequency. Q is the activation energy, V is the activation volume, R is the gas constant and T is the absolute temperature. τ^* is the shear stress acting on the deformation mechanism and is related to the applied stress by

$$\tau^* = \frac{\sigma^*}{\overline{m}} \tag{3}$$

where $\overline{m}$ is an orientation factor with the approximate value of 3.[16] $V\tau^*$ is defined as the total work done by the stress during the rate-controlling event.[14]

If A, Q and V are assumed constant, Equation (2) can be combined with Equations (1) and (3) and integrated to give an expression of the form[12]

$$\sigma - \sigma_o = B - D \log (t + C)$$

where B, C and D are constants. This equation is the one commonly used to interpret logarithmic stress relaxation in terms of operating deformation mechanisms. As we have shown in the present work on PZT and others have shown for $BaTiO_3$[5] this analysis cannot be used to interpret stress-relaxation data observed with these materials. Reed-Hill and Dahlberg[17] have, however, developed an analysis of stress relaxation kinetics in anelastic materials based on the concepts of thermally activated deformation that can be used to interpret the data shown in Figure 4 and 5. A slightly modified form of this analysis is briefly described in what follows.

In Equation (2) only forward activation of the deformation mechanism was considered. If forward and reverse activation are allowed the relaxable strain rate is

$$\dot{\epsilon}^* = A\left[e^{-\frac{(Q - V\tau^*)}{RT}} - e^{-\frac{(Q + V\tau^*)}{RT}}\right] \tag{4}$$

where the second term accounts for the strain rate contribution due to reverse motion of the deformation mechanism. This fundamental expression in reaction rate theory[18] was applied to thermally activated deformation by Kuhlman[17, 19] who treated only the limiting cases of short and long time periods. Reed-Hill and Dahlberg[17] have extended the analysis to include intermediate times thereby making the treatment valid over a wider range of strains. Equation (4) may be written as:

$$\dot{\epsilon}^* = 2Ae^{-\frac{Q}{RT}} \sinh \frac{V\tau^*}{RT} \tag{5}$$

Since the relaxable strain rate is given by Equation (1), combining equations (1), (3) and (4) gives

$$\frac{\dot{\sigma}^*}{M_u} = -2Ae^{-\frac{Q}{RT}} \sinh \frac{\beta\sigma^*}{RT} \tag{6}$$

where $\beta = \frac{V}{\overline{m}}$.

We should point out at this time that this analysis differs slightly from that of Reed-Hill and Dahlberg.[17] In the latter, only a fraction of the effective stress was considered to relax. The amount that relaxed was given by an expression of Zener's.[6]

$$\sigma_{relax} = (\sigma - \sigma_{t=\infty}) = \frac{\overline{m}\,(M_u - M_r)}{M_u}\,\tau^*$$

where M_u and M_r are the unrelaxed and relaxed moduli respectively and τ^* is the effective shear stress acting on the deformation mechanism. $\sigma_{t=\infty}$ is the totally relaxed stress. If the relaxable stress is given by the above then β in Equation (6) is as follows:

$$\beta = \frac{V M_u}{\bar{m} (M_u - M_r)}$$

Recent work[11, 20] has indicated that the relaxed stress at $t = \infty$ is the internal stress, σ_G, and that it can be measured by long time relaxation runs or by the incremental unloading technique discussed earlier. In this report we adapt this suggestion and treat the relaxable stress $(\sigma - \sigma_{t=\infty})$ as being equivalent to the effective stress $\sigma^* = (\sigma - \sigma_G)$.

Integrating Equation (6) with respect to time gives

$$\log \tanh \frac{\beta\sigma^*}{2RT} = -\frac{\tau}{\tau_\epsilon} + C \qquad (7)$$

where C is a constant of integration and the relaxation time, τ_ϵ, defined by

$$\frac{1}{\tau_\epsilon} = \frac{2M_u\beta}{RT} A e^{-\frac{Q}{RT}} \qquad (8)$$

For small values of $\frac{\beta\sigma^*}{2RT}$, Equation (7) reduces to the equation for logarithmic stress relaxation. Stress relaxation data such as those shown in Figures 4 and 5 can be analyzed in terms of these equations by plotting log tanh $\frac{\beta\sigma^*}{2RT}$ versus time. A linear relation is obtained by varying β and using it as a fitting parameter. Since $\bar{m}$ is a constant this amounts to determining the value of the activation volume consistent with each stress relaxation curve. The effective stresses, σ^*, used in the plots are the differences between the instantaneous applied stresses, corrected for machine relaxation, and the internal stress determined at each temperature by the incremental unloading technique.

Most data discussed in what follows were obtained from stress relaxation runs made on PZT from an initial stress level of approximately 65.5 MPa (9500 psi). The internal stresses measured by incremental unloading from this stress level are shown in Figure 6 as a function of temperature. Note that the internal stress in PZT is linear with temperature over the temperature range examined. It was also found that the internal stresses increased linearly with initial stress level.

The curve-fitting procedure discussed above is shown in Figure 7 for stress relaxation data taken at room temperature and at 71°C. The figure shows $\log \tanh \frac{\beta\sigma^*}{2RT}$ plotted as a function of time. Each curve on the figure represents the data plotted with a different value of β. At room temperature a linear fit was obtained at a value of $\beta = 90$ and at 71°C the fit occurred at $\beta = 40$. Activation volumes calculated in this manner using Equation (7) and stress relaxation data taken at room temperature, 34°, 52° and 71°C are shown in Figure 8. Stress relaxation data taken from different initial stress levels at room temperature were also run to determine the dependence of the activation volume on effective stress. Figure 9 shows that the activation volume varies linearly with effective stress.

As noted in Equation (8), the activation energy, Q, of the rate-controlling deformation mechanism can be obtained from the slope of a linear plot of $\log \frac{\tau_\varepsilon \beta}{T}$ versus $\frac{1}{T}$. The relaxation times used in the plot are obtained, according to Equation (7) from the best-fit linear curves to data such as those shown in Figure 7. The activation energy calculation is a significant step in the analysis. If a single mechanism is rate controlling and the analysis is valid, then a plot of $\log \frac{\tau_\varepsilon \beta}{T}$ versus $\frac{1}{T}$ should be linear and the value of Q can be calculated. If not, the analysis is not applicable. As shown in Figure 10 the plot is linear for the data taken on PZT and the experimental activation energy is 25 Kcal/mole. The error bars on the plot correspond to the total data spread at each temperature. Two runs were made at each of the two high temperatures, four runs were made at 34°C and three runs were made at room temperature.

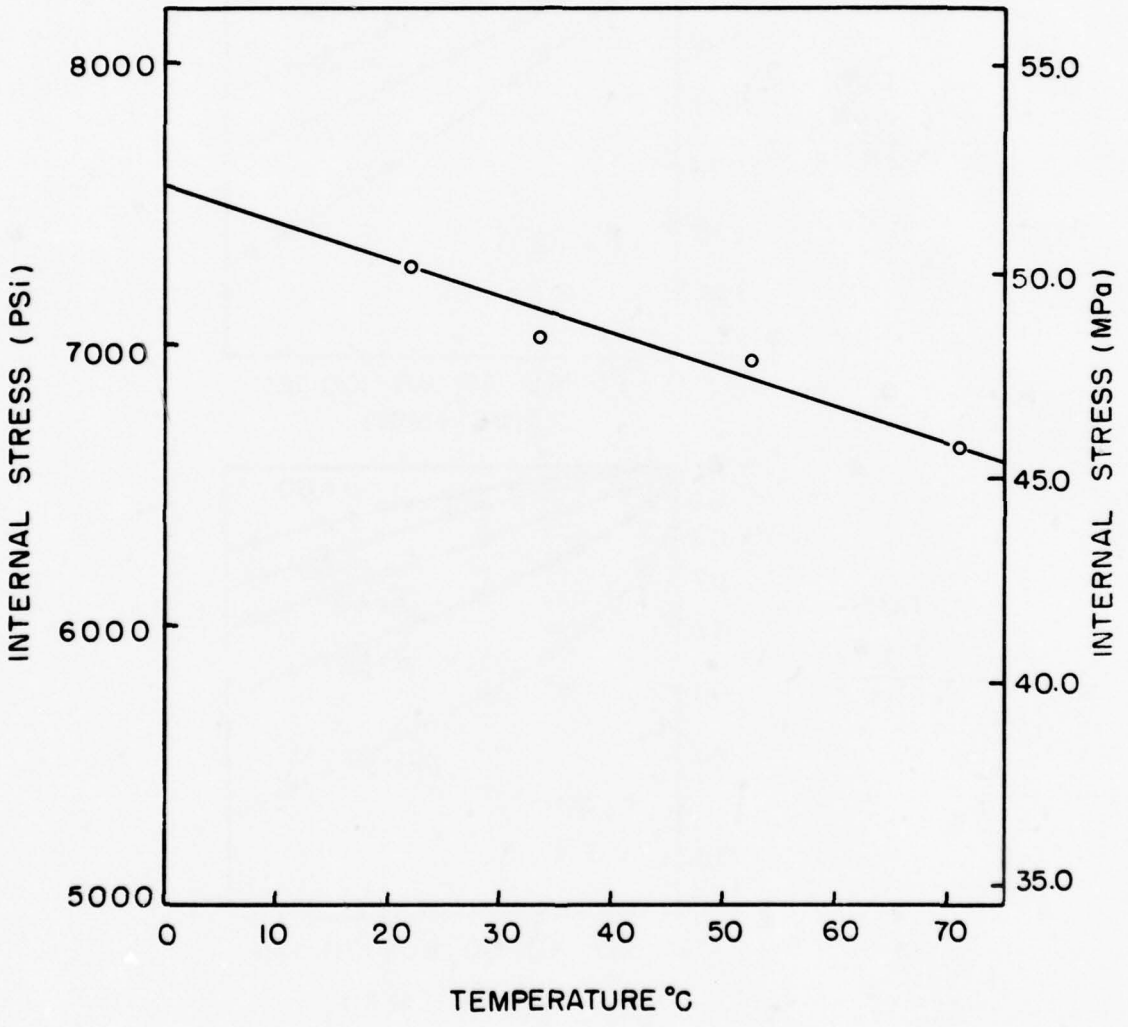

Figure 6. Variation of the Internal Stress as Measured by the Incremental Unloading Technique From an Initial Stress Level of 65.5 MPa With Temperature

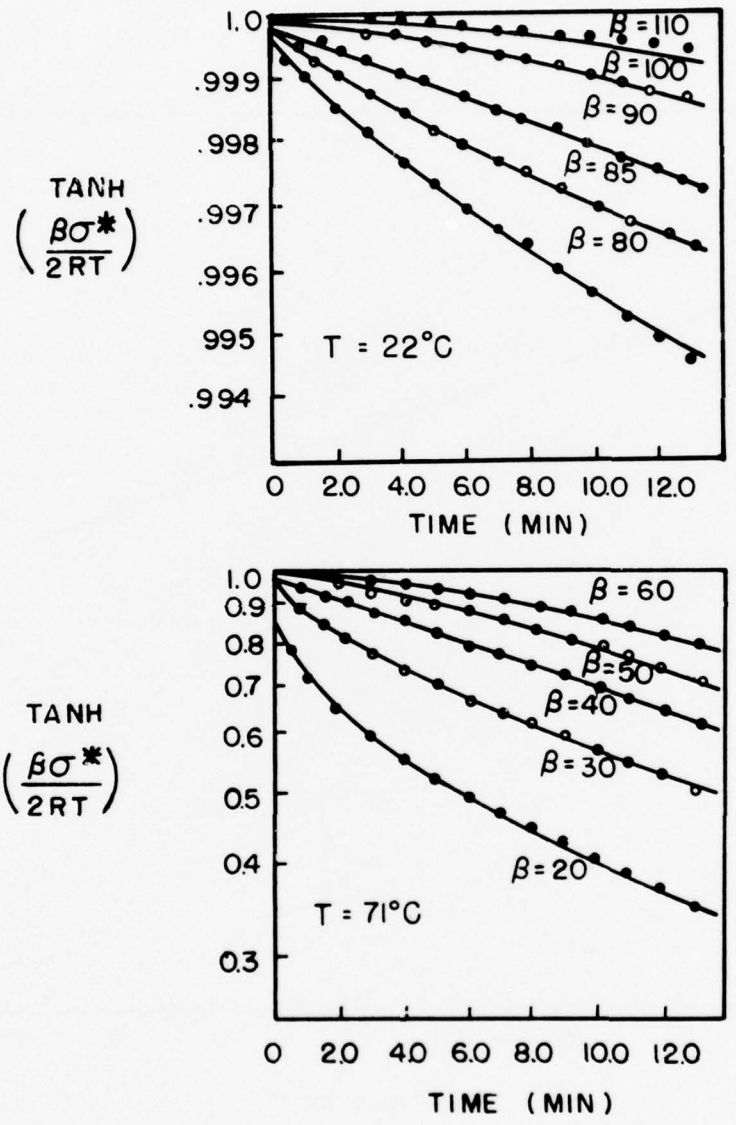

Figure 7. Log Tanh $(\frac{\beta\sigma^*}{2RT})$ Plotted as a Function of Time at Two Temperatures. A linear fit to the relaxation data obtains with β = 90 at room temperature and with β = 40 at 71°C.

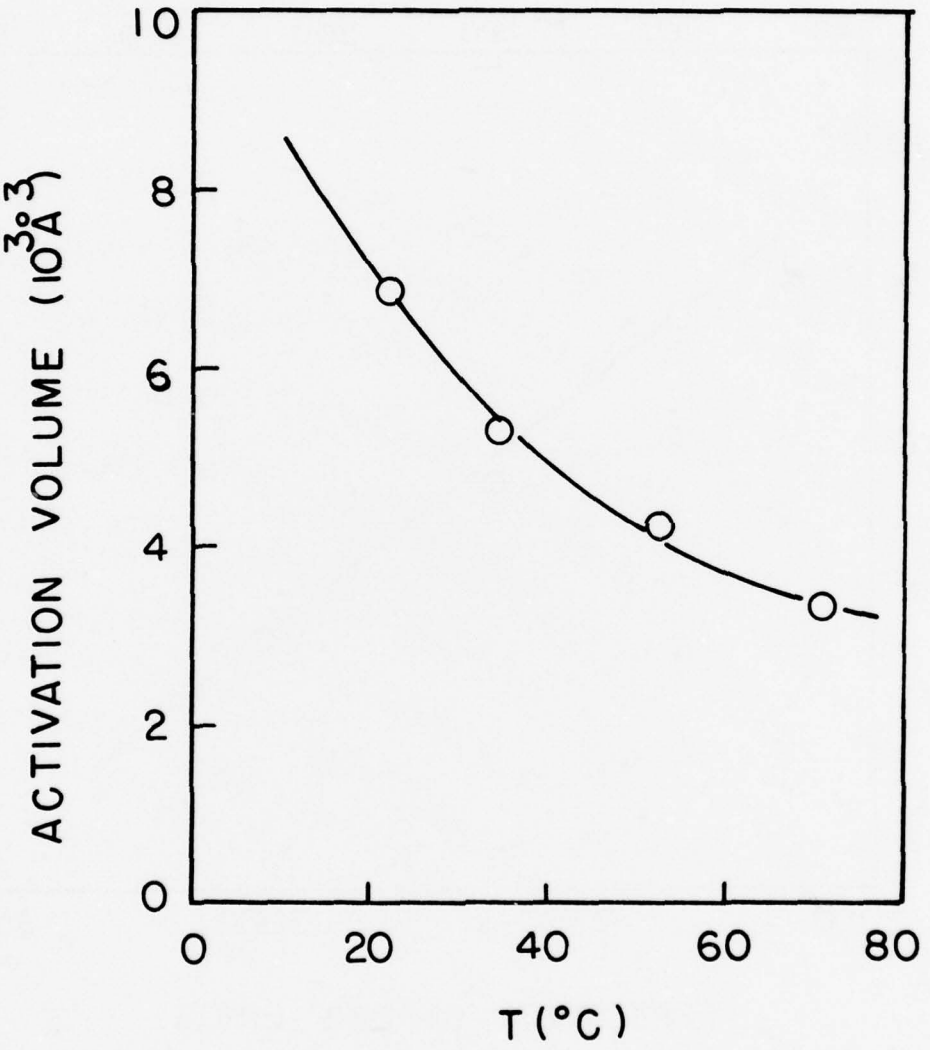

Figure 8. Temperature Dependence of the Activation Volume Measured from Stress Relaxation Data Taken from an Initial Stress of 65.5 MPa

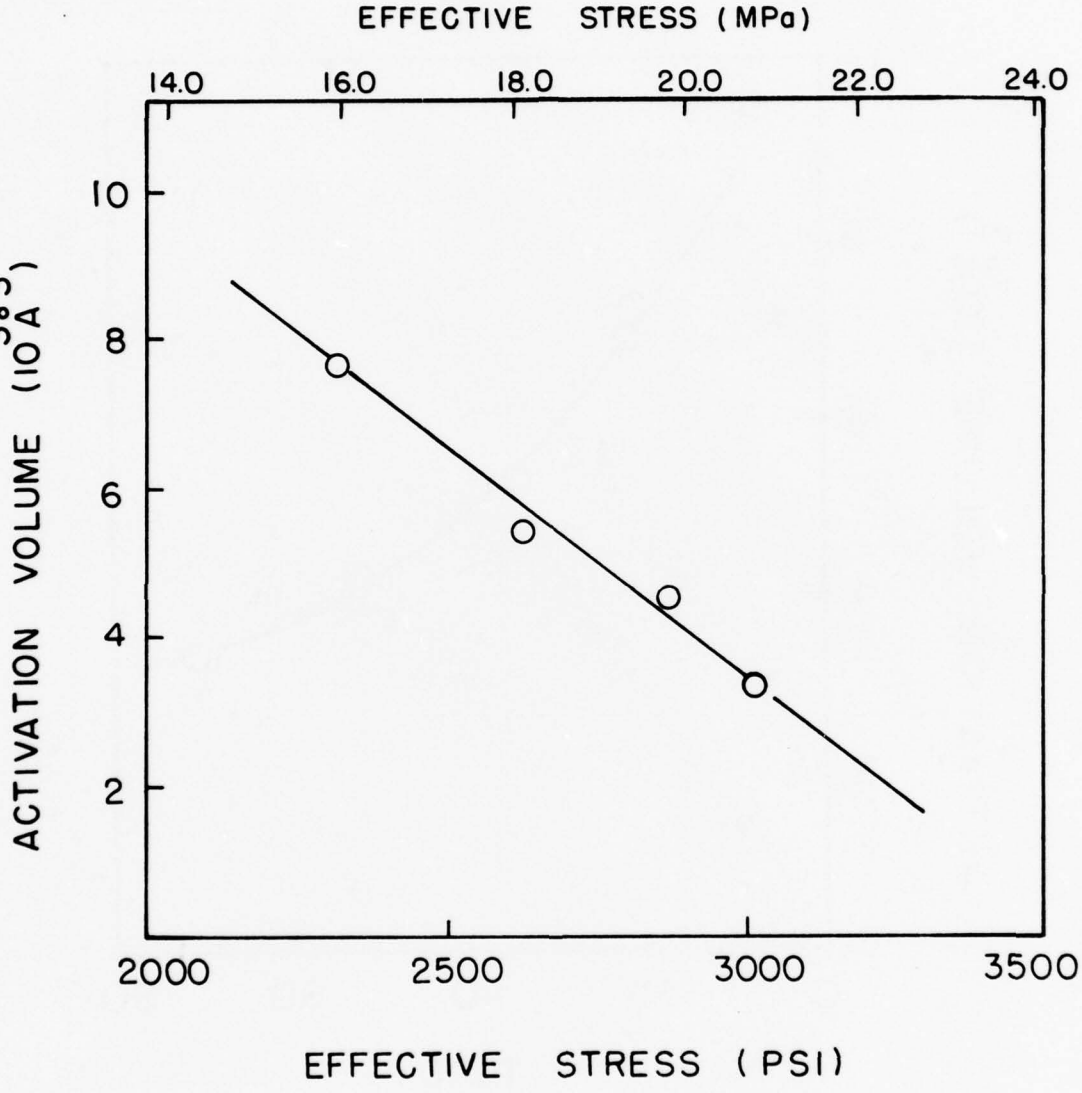

Figure 9. Activation Volume for PZT Plotted as a Function of the Effective Stress at Room Temperature

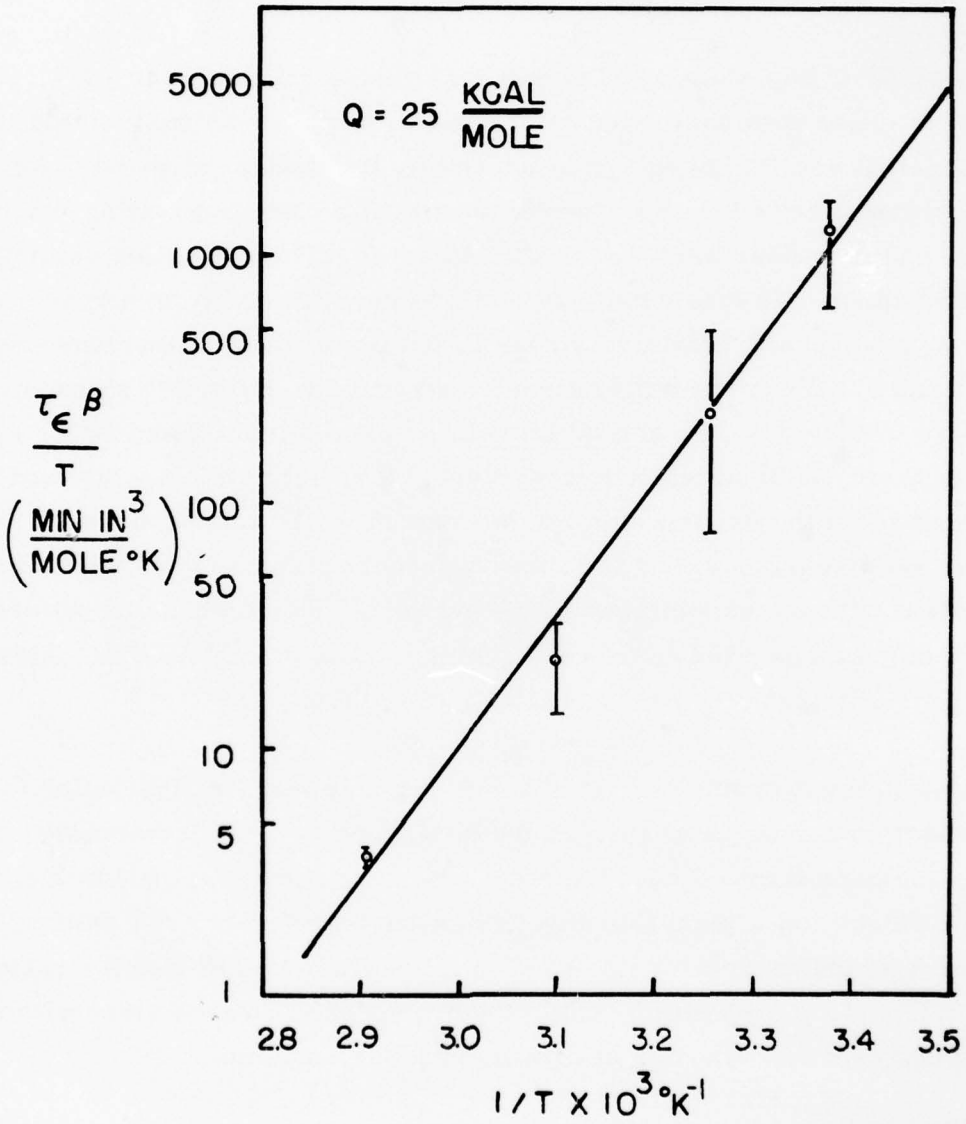

Figure 10. Log $\frac{\tau \epsilon \beta}{T}$ Plotted versus $\frac{1}{T}$ for PZT. The experimental activation energy is ≃ 25 kcal/mole.

V. A MODEL OF TIME-DEPENDENT DEFORMATION IN PZT

The results of this study have shown that stress relaxation in PZT, although not logarithmic with time, can be treated in terms of an analysis developed by Reed-Hill and Dahlberg[17] that presumes thermally activated deformation occurs by both forward and reverse motion of a rate-controlling deformation mechanism over barriers in the material. The activation volume of the mechanism was measured and found to decrease with temperatue and to vary linearly with effective stress in the stress and temperature ranges investigated. When the initial stress for stress relaxation was about 65.5MPa (9500 psi), the activation volume varied from about 3000Å at 71°C to about 7000Å at room temperature. The activation energy was determined from the experimental data to be 25 kcal/mole (1.09 ev). In what follows we discuss a model for time-dependent deformation in PZT that is consistent with the experimental observations. The discussion differs from those usually used to describe deformation in piezoelectric materials[1,2,5,7] in that it is based on dislocation theory.

As noted in the Introduction, it is a well-established fact that deformation in piezoelectric ceramics occurs by domain processes. Furthermore, the particular processes involved are the stress (mechanical and/or electrical)-induced migration of non-180-degree domain boundaries. We further emphasize that the measurements made in this study relate to the kinetics of domain boundary migration. The model discussed is consistent with both the mechanism and kinetics of domain boundary motion.

It is important to point out that non-180-degree domain boundaries in piezoelectric ceramics are twin boundaries[8] and that the deformation associated with boundary migration is a twinning shear. In tetragonal PZT, spontaneous polarization is along the c-axis and the domain (i.e., twin) boundary is

a {110} plane. The twinning shear associated with the boundary is in the $\langle\bar{1}10\rangle$ direction as shown in Figure 11. The dotted lines on the figure show the position of a tetragonal unit cell after twinning has occurred. The cell axes before twinning are denoted **c** and **a** and those after twinning are denoted **c'** and **a'**. In rhombohedral PZT spontaneous polarization is along the <111> directions. One of the twinning shears associated with a domain boundary in the rhombohedral phase is also shown in Figure 11. The twin plane is {110} and the twinning shear is in the <001> direction. Since the PZT examined in this work is predominantly tetragonal, we will limit our discussion to twinning in that phase. At temperatures below the Curie temperature, polycrystalline piezoelectric ceramics contain a high density of ferroelectric domains.[8] The domains (i.e., twins) form to accomodate the strain associated with the cubic to tetragonal (or rhombohedral) phase transformation occurring at the Curie temperature. Since the stress to nucleate new twins is presumably higher than that necessary to propagate existing ones[20] deformation in these materials occurs predominantly by the migration of existing domain boundaries. The heavily twinned structure also accounts for the observation that time-dependent deformation in piezoelectric ceramics can occur at the relatively low stress levels shown in Figure 4.

A number of dislocation models for twin (i.e., domain) boundary migration exist – the most prominent being the pole mechanism of Cottrell and Bilby.[21,22] Since the pole mechanism requires high dislocation mobility and intricate mutual dislocation interactions, its application as a low-temperature source of twinning dislocations in oxide ceramics is unlikely. A more plausible source of twinning dislocations in ceramic PZT is the homogeneous nucleation of twinning dislocation loops as proposed by Birnbaum and Read.[23] In this mechanism a twin boundary propagates by the successive nucleation of twinning dislocation loops on the lattice plane just in front of the moving twin boundary. Ordinarily the high strain energy associated with a dislocation would make homogenous nucleation of a loop highly

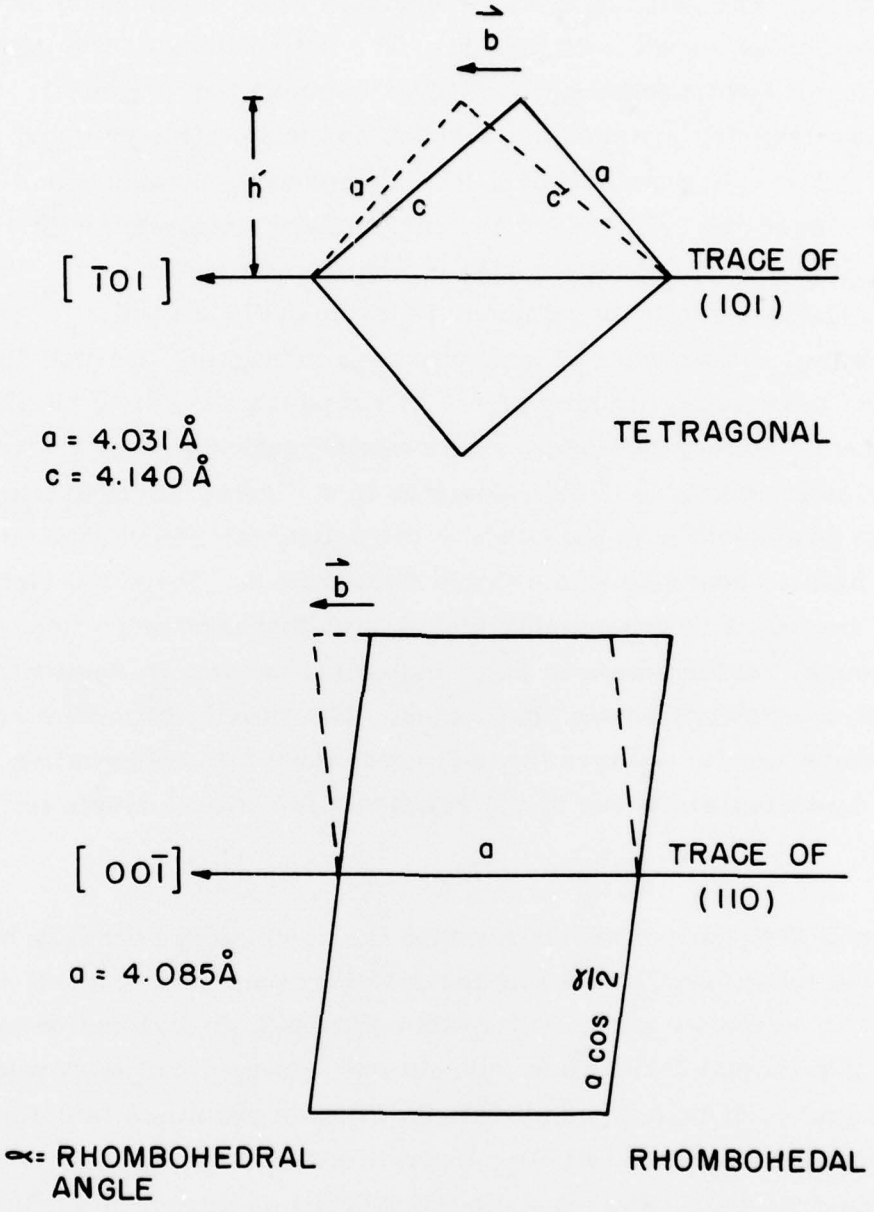

Figure 11. Schematic Showing the Geometry of Twinning in PZT

unlikely. Stresses on the order of the theoretical shear strength are required.[24] A twinning dislocation, on the other hand, has a Burgers vector that is only a fraction of the size of a rational lattice vector. Since the strain energy is proportional to the square of the Burgers vector the energy of a twinning dislocation is correspondingly lower. The Burgers vector for the twinning shear in tetragonal PZT is only 0.154Å.

The activation energy, U_c, and critical stress, σ_c, required to homogeneously nucleate a twinning dislocation loop with a radius of r_c in PZT may be calculated from expressions given by Cottrell[23,24]

$$U_c = \frac{Gb^2 r_c}{4}\left[\ln\left(\frac{r_c}{r_o}\right) - 1\right]$$

$$\sigma_c = \frac{Gb}{4\pi r_c}\left[\ln\left(\frac{r_c}{r_o}\right) + 1\right]$$

where G is the shear modulus, b is the magnitude of the Burgers vector and $r_o = \frac{b}{4}$.[25] Taking $G = 2.56 \times 10^4$ MPa[26] and the experimentally determined activation energy, a loop radius of 160Å is calculated. This corresponds to a critical stress of 18.3MPa (2653 psi). Both the size of the loop and the critical stress are reasonable values. The activation volume can be estimated from the size of the twinning dislocation loop according to

$$V = \pi r_c^2 b \simeq 12{,}400\text{Å}^3$$

This value is within a factor of two of the experimentally measured activation volumes.

VI. CONCLUSIONS

Stress relaxation in PZT has been found to occur at relatively low values of stress and to depend systematically on both stress and temperature. The stress and temperature dependence of the relaxation behavior suggest that the deformation mechanism is thermally activated. The data only exhibit logarithmic stress relaxation over a fraction of the time intervals used in the tests and cannot be analyzed in terms of the usual Ahrennius equation. An analysis by Reed Hill and Dahlberg[17] was successfully applied to the results and an experimental activation energy and activation volume of 25 kcal/mole and 3,000 to 7,000Å respectively were measured. The accepted deformation mechanism for piezoelectric ceramics is non-180 degree domain boundary migration. Since non-180 degree domain boundaries are twin boundaries, a dislocation model for twin boundary migration is presented that is quite consistent with the experimental activation parameters. The data strongly suggest that domain boundary migration in PZT occurs by the homogenous nucleation of twinning dislocation loops on lattice planes immediately adjacent to the boundary.

VII. ACKNOWLEDGEMENTS

The authors are indebted to Dr. R.J. Stokes and S. Schuldt for helpful and critical discussion and to S.J. Tibbetts and D.W. Woodward for experimental assistance during the course of this work. W.B. Harrison of the Honeywell Ceramics Center graciously supplied the PZT. The continued interest of Dr. R.C. Pohanka, Office of Naval Research, is gratefully acknowledged.

VIII. REFERENCES

1. E.C. Subbarao, M.C. McQuarrie and W.R. Buessem, "Domain Effects in Polycrystalline Barium Titanate," J. Appl. Phys., 28 [10] 1194-1200 (1957).

2. L.N. Syrkin and A.M. Elgard, "Influence of the Domain Structure of Ceramic Ferroelectrics on Their Mechanical Properties," Sov. Phys. Sol. State, 7, [4] 967-71 (1965).

3. V.C.S. Prasad and E.C. Subbarao, "Deformation Studies in $BaTiO_3$ Single Crystals," Appl. Phys. Lett., 22 [8] 424-25 (1973).

4. V.C.S Prasad and E.C. Subbarao, "Stress Relaxation Study of Ferroelectric Domains," Ferroelectrics, 7 [1-2] 311 (1974) (Abstract Only).

5. V.C.S Prasad and E.C. Subbarao, "Deformation and Stress Relaxation of Single Crystal $BaTiO_3$," Ferroelectrics, 15 [3-4] 143-148 (1977).

6. C. Zener, Elasticity and Anelasticity of Metals, University of Chicago Press, Chicago, 1948.

7. D. Berlincourt and H.H.A. Krueger, "Domain Processes in Lead Titanate Zirconate and Barium Titanate Ceramics," J. Appl. Phys., 30 [11] 1804-10 (1959).

8. B. Jaffe, W.R. Cook and H. Jaffe, Piezoelectric Ceramics, Academic Press, New York, 1971.

9. J.G. Bruce and B.G. Koepke, "Crack Propagation in PZT," Honeywell Corporate Material Sciences Center, First Technical Report to the Office of Naval Research on Contract No. N00014-76-C-0625/P00002 (1977).

10. J.G. Bruce, W.W. Gerberich and B.G. Koepke, pp. 687-709 in Fracture Mechanics of Ceramics, Vol. 4. Edited by R.C. Bradt D.P.H. Hasselman and F.F. Lange, Plenum Press, New York, 1978.

11. S.R. MacEwen, O.A. Kupcis and B. Ramaswami, "An Investigation of an Incremental Unloading Technique for Estimating Internal Stress," Scripta Met., 3 [7] pg. 441-48 (1969).

12. F. Guiu and P.L. Pratt, "Stress Relaxation and the Plastic Deformation of Solids," Phys. Stat. Sol., 6 [1] 111-120 (1964).

13. A.G. Evans and R.D. Rawlings, "The Thermally Activated Deformation of Crystalline Materials," Phys. Stat. Sol., 34 [1] 9-31 (1969).

14. G.B. Gibbs, "The Thermodynamics of Thermally-Activated Dislocation Glide," Phys. Stat. Sol., 10 [2], 507-12 (1965).

15. U.F. Kocks, A.S. Argon and M.F. Ashby, "Thermodynamics and Kinetics of Slip," Prog. Mater. Sci., 19, 1-288 (1975).

16. C.N. Reid, Deformation Geometry for Materials Scientists, Pergamon Press, New York, pg. 171.

17. R.E. Reed-Hill and E.P Dahlberg, "Concerning the Relaxation of Strain at Constant Stress and the Relaxation of Stress at Constant Strain," Trans. Met. Soc. AIME, 236, [5], 679-85 (1966).

18. D. Kuhlman, Z. Phys., 124, pp. 468-81 (1947).

19. E.O. Hall, Twinning and Diffusionless Transformations in Metals, Butterworths, London, 1954, pg. 119-20.

20. A.H. Cottrell and B.A. Bilby, Phil. Mag., 42, [329], 573-81, (1951).

21. J.P. Hirthe and J. Lothe, Theory of Dislocations, McGraw-Hill, New York, 1968, pg. 743.

22. H.K. Birnbaum and T.A. Reed, Trans. Met. Soc. AIME, 218 [4], 662-69, (1960).

23. A.H. Cottrell, Dislocations and Plastic Flow in Crystals, Clarendon Press, Oxford, 1953, pg. 53.

24. J.P. Hirthe and J. Lothe, Loc. Cit., pg. 138.

25. B. Jaffe, W.R. Cook and H. Jaffe, Loc. Cit., pg. 146.

BASIC DISTRIBUTION LIST October 1978

Technical and Summary Reports

Organization	No. of Copies
Defense Documentation Center Cameron Station Alexandria, Virginia 22314	(12)
Office of Naval Research Department of the Navy	
Attn: Code 471	(1)
Code 102	(1)
Code 470	(1)
Commanding Officer Office of Naval Research Branch Office 495 Summer Street Boston, Massachusetts 02210	(1)
Commanding Officer Office of Naval Research Branch Office 536 South Clark Street Chicago, Illinois 60605	(1)
Office of Naval Research San Francisco Area Office 760 Market Street, Room 447 San Francisco, California 94102 Attn: Dr. P. A. Miller	(1)
Naval Research Laboratory Washington, D.C. 20390	
Attn: Code 6000	(1)
Code 6100	(1)
Code 6300	(1)
Code 6400	(1)
Code 2627	(1)
Naval Air Development Center Code 302 Warminster, Pennsylvania 18974 Attn: Mr. F. S. Williams	(1)
Naval Air Propulsion Test Center Trenton, New Jersey 08628 Attn: Library	(1)
Naval Construction Batallion Civil Engineering Laboratory Port Hueneme, California 93043 Attn: Materials Division	(1)
Naval Electronics Laboratory Center San Diego, California 92152 Attn: Electron Materials Sciences Division	(1)
Naval Missile Center Materials Consultant Code 3312-1 Point Mugu, California 93041	(1)
Commanding Officer Naval Surface Weapons Center White Oak Laboratory Silver Spring, Maryland 20910 Attn: Library	(1)
David W. Taylor Naval Ship R&D Center Materials Department Annapolis, Maryland 21402	(1)
Naval Undersea Center San Diego, California 92132 Attn: Library	(1)
Naval Underwater System Center Newport, Rhode Island 02840 Attn: Library	(1)
Naval Weapons Center China Lake, California 93555 Attn: Library	(1)
Naval Postgraduate School Monterey, California 93940 Attn: Mechanical Engineering Dept.	(1)
Naval Air Systems Command Washington, D.C. 20360	
Attn: Code 52031	(1)
Code 52032	(1)
Code 320	(1)

BASIC DISTRIBUTION LIST (Cont'd) October 1978

Organization	No. of Copies
Naval Sea System Command Washington, D.C. 20362 Attn: Code 035	(1)
Naval Facilities Engineering Command Alexandria, Virginia 22331 Attn: Code 03	(1)
Scientific Advisor Commandant of the Marine Corps Washington, D.C. 20380 Attn: Code AX	(1)
Naval Ship Engineering Center Department of the Navy CTR BG #2 3700 East-West Highway Prince Georges Plaza Hyattsville, Maryland 20782 Attn: Engineering Materials and Services Office, Code 6101	(1)
Army Research Office Box CM, Duke Station Durham, North Carolina 27706 Attn: Metallurgy & Ceramics Div.	(1)
Army Materials and Mechanics Research Center Watertown, Massachusetts 02172 Attn: Res. Programs Office (AMXMR-P)	(1)
Air Force Office of Scientific Research Bldg. 410 Bolling Air Force Base Washington, D.C. 20332 Attn: Chemical Science Directorate Electronics and Solid State Sciences Directorate	(1) (1)
Air Force Materials Lab (LA) Wright-Patterson AFB Dayton, Ohio 45433	(1)

Organization	No. of Copies
NASA Headquarters Washington, D.C. 20546 Attn: Code RRM	(1)
NASA Lewis Research Center 21000 Brookpark Road Cleveland, Ohio 44135 Attn: Library	(1)
National Bureau of Standards Washington, D.C. 20234 Attn: Metallurgy Division Inorganic Materials Division	(1) (1)
Defense Metals and Ceramics Information Center Battelle Memorial Institute 505 King Avenue Columbus, Ohio 43201	(1)
Director Ordnance Research Laboratory P.O. Box 30 State College, Pennsylvania 16801	(1)
Director Applied Physics Laboratory University of Washington 1013 Northeast Fortieth Street Seattle, Washington 98105	(1)
Metals and Ceramics Division Oak Ridge National Laboratory P.O. Box X Oak Ridge, Tennessee 37380	(1)
Los Alamos Scientific Laboratory P.O. Box 1663 Los Alamos, New Mexico 87544 Attn: Report Librarian	(1)
Argonne National Laboratory Metallurgy Division P.O. Box 229 Lemont, Illinois 60439	(1)

BASIC DISTRIBUTION LIST (Cont'd)

Organization	No. of Copies
Brookhaven National Laboratory Technical Information Division Upton, Long Island New York 11973 Attn: Research Library	(1)
Library Building 50 Room 134 Lawrence Radiation Laboratory Berkeley, California	(1)

TP
October 1978

SUPPLEMENTARY DISTRIBUTION LIST

Technical and Summary Reports

Advanced Research Projects Agency
Materials Science Director
1400 Wilson Boulevard
Arlington, VA 22209

Professor Michael Bell
Yeshiva University
Belfer Graduate School of Science
New York, NY 10033

Dr. Don Berlincourt
Channel Products
16722 Park Circle Dr. W.
Chagrin Falls, OH 44022

Dr. J. V. Biggers
Pennsylvania State University
Materials Research Laboratory
University Park, PA 16802

Mr. George Boyer
Sensor Systems Program
Office of Naval Research
Code 222
Arlington, VA 22217

Professor R. Bradt
Ceramics Section
Materials Sciences Department
The Pennsylvania State University
University Park,, PA 16802

Dr. Dean Buckner
Piezo Products Division
Gulton Industries
P.O. Box 4300
Fullerton, CA 92634

Dr. Robert Callahan
Channel Industries
839 Ward Drive
Box 3680
Santa Barbara, CA 93105

Professor L. E. Cross
The Pennsylvania State University
Materials Research Laboratory
University Park, PA 16802

Mr. N. Coda
Vice President for Engineering
Erie Technological Products
West College Avenue
State College, PA 1680

Dr. A. G. Evans
Rockwell International
P.O. Box 1085
1049 Camino Dos Rios
Thousand Oaks, CA 91360

Dr. Richard Fulrath
University of California
266 Hearst Mining Building
Berkeley, CA 94720

Dr. Gene Haertling
Motorola Corporation
3434 Vassar, NE
Albuquergue, NM 87107

Mr. W. B. Harrison
Honeywell Ceramics Center
1885 Douglas Drive
Golden Valley, MN 55422

Dr. D. P. H. Hasselman
Virginia Polytechnic Institute
Department of Materials Sciences
Blacksburg, VA

Dr. L. L. Hench
Department of Metallurgy
University of Florida
Gainesville, FL 32603

Dr. A. H. Heuer
Professor of Ceramics
Case Western Reserve University
University Circle
Cleveland, OH 44106

Dr. F. Robert Hill
Marine Resources
755 Highway 17 & 92
Fern Park, FL 32730

SUPPLEMENTARY DISTRIBUTION LIST (CONT"D)

Dr. Bernard Jaffe
232 Forbes Road
Bedford, OH 44146

Dr. Paul Jorgensen
Stanford Research Institute
333 Ravenswood Avenue
Menlo Park, CA 94025

Dr. R. N. Katz
Army Materials and Mechanics
Research Center
Watertown, MA 02172

Dr. H. Kirchner
Ceramic Finishing Company
P. O. Box 498
State College, PA 16801

Dr. B. G. Koepke
Honeywell, Inc.
Corporate Research Center
10701 Lyndale Avenue South
Bloomington, MN 55420

Mr. Frank Koubek
Naval Surface Weapons Center
White Oak Laboratory
Silver Spring, MD 20910

Dr. J. Lankford
Southwest Research Institute
8500 Culebra Road
San Antonio, TX 78284

Dr. R. Lapetina
Edo Western Corporation
2645 South 300 West
Salt Lake City, UT 84115

Mr. C. LeBlanc
Naval Underwater Systems Center
TD 121
Newport, RI 02840

Dr. R. E. Loehman
University of Florida
Ceramics Division
Gainesville, FL 32601

Professor P. B. Macedo
The Catholic University of America
Washington, DC 20017

Dr. N. Perrone
Code 474
Office of Naval Research
800 N. Quincy Street
Arlington, VA 22217

Dr. R. Pohanka
Naval Research Laboratory
Code 6130
Washington, DC 20375

Dr. R. Rice
Naval Research Laboratory
Code 6360
Washington, DC 20375

Dr. Frank Recny
General Electric Company
Court Street
Plant Building C
Box 1122
Syracuse, NY 13201

Dr. J. H. Rosolowski
General Electric Company
Research and Development Center
P.O. Box 8
Schenectady, NY 02301

Dr. D. A. Shockey
Stanford Research Institute
Poulter Laboratory
Menlo Park, CA 94025

Dr. J. H. Simmons
Catholic University of America
Washington, DC 20064

Dr. P. L. Smith
Naval Research Laboratory
Code 6361
Washington, DC 20375

SUPPLEMENTARY DISTRIBUTION LIST (CONT'D)

Dr. R.W. Timme
Naval Research Laboratory
Code 8275
Underwater Sound Reference Division
P.O. Box 8337
Orlando, FL 32806

Dr. Charles C. Walker
Naval Sea Systems Command
National Center #3
2531 Jefferson Davis Highway
Arlington, VA 20390

Dr. Paul D. Wilcox
Sandia Laboratories
Division 2521
Albuquerque, NM 87115

The State University of New York
at Alfred
Material Sciences Division
Alfred, NY 14802

Dr. N.S. Corney
Ministry of Defense
(Procurement Executive)
The Adelphi
John Adam Street
London WC2N 6BB
UNITED KINGDOM

Dr. Murray Gillen
Australian Embassy
Washington, DC 33801

Dr. D.J. Godfrey
Admiralty Materials Laboratory
Ministry of Defense
(Procurement Executive)
Holton Heath
Poole, Dorset
BH16 6JU
UNITED KINGDOM

Linda Husted
Librarian
Materials Sciences Corporation
Merion Towle Building
Blue Bell, PA 19422

Globe-Union, Inc.
5757 North Green Bay Avenue
Milwaukee, WI 53201
ATTN: G. Goodman

Prof. P.J. Gielisse
Dept. of Chemical Engineering
University of Rhode Island
Kingston, RI 02881

Dr. M. Noone
General Electric Company
Space Sciences Laboratory
Room M9539, P.O. Box 8555
Philadelphia, PA 19101

Dr. R.N. Katz
Army Mechanics and Materials
Research Center
Watertown, MA 02172

Mr. W.B. Crandall
Alfred University
Alfred, NY 14802

Dr. J.T.A. Roberts
Electric Power Research Institute
3412 Hillview Ave.
P.O. Box 10412
Palo Alto, CA 94303

Dr. W.R. Manning
Champion Spark Plug Company
20000 Conner Ave.
Detroit, MI 48234

Dr. G.K. Bansal
Battelle
505 King Avenue
Columbus, OH 43201

Dr. B.A. Wilcox
Ceramics Program, Room 336
Metallurgy and Materials Research
National Science Foundation
Washington, D.C. 20550

Dr. H.E. Bennett
Naval Surface Weapons Center
Research Department Code 601
China Lake, CA 93555

SUPPLEMENTARY DISTRIBUTION LIST (CONT'D)

Dr. R.J. Charles
General Electric Company
Research and Development Center
Schenectady, NY 12301

Dr. A.R.C. Westwood
Martin-Marietta Laboratories
1450 South Rolling Road
Baltimore, MD 21227

Professor R.H. Doremus
Rensselaer Polytechnic Institute
Troy, NY 12181

Dr. D.E. Niesz
Battelle Memorial Institute
505 King Avenue
Columbus, OH 43201

Dr. S.M. Wiederhorn
Inorganic Materials Division
National Bureau of Standards
Washington, D.C. 20234

Dr. C.O. Hulse
United Aircraft Research Labs
United Aircraft Corporation
East Hartford, CT 06108

Prof. M.H. Manghnani
University of Hawaii
Hawaii Institute of Geophysics
2525 Correa Road
Honolulu, HI 96822

Dr. Marvin Hass
Naval Research Laboratory
Code 6408
Washington, D.C. 20375

Dr. S.M. Wiederhorn
Physical Properties Section
Bldg. 223, Rm. A355
National Bureau of Standards
Washington, D.C. 20234

Dr. P.F. Becher
Code 6362
U.S. Naval Research Laboratory
Washington, D.C. 20375